5th International Congress
of Croatian Society of Mechanics
September, 21-23, 2006
Trogir/Split, Croatia

PROJECTIVE CONSTRAINT VIOLATION STABILIZATION METHOD FOR MULTIBODY SYSTEMS ON MANIFOLDS

Zdravko Terze, Joris Naudet

Keywords: *Constrained mechanical systems, Numerical integration on manifolds, Dynamic simulation of multibody systems*

ABSTRACT

Constraint gradient projective method for stabilization of constraint violation during time integration of multibody systems (MBS) is in focus of the paper. Mathematical model for constrained MBS dynamic simulation on manifolds is introduced and numerical violation of system kinematical constraints is discussed. As an extension of the previous work, that was focused on time integration of holonomic systems, the stabilization projective method is discussed in the context of generally constrained mechanical systems. By adopting differential-geometric point of view, the geometric and stabilization issues of the method are addressed. After discussing optimization of partitioning algorithm, it is shown that the projective stabilization method can be applied for numerical stabilization of holonomic and non-holonomic constraints in Pfaffian and general form.

1. INTRODUCTION

During dynamical simulation of constrained multibody systems, a violation of system kinematical constraints is the basic source of time-integration errors and frequent difficulty that analyst have to cope with. Baumgarte stabilization method that minimizes violations can be applied for this purpose, but this algorithm is dependent on empirical feedback gains and has some limitations [1]. Different methods that provide full stabilization of system constraints are discussed in [2]. The stabilized integration procedure, whose stabilization step is based on projection of the integration results to the underlying constraint manifold *via* post-integration correction of selected coordinates, is proposed and compared with similar integration schemes in [3]. The integration procedure is compatible with many ODE integrators and provides full stabilization of system constraint violation, but its utilization is confined to the holonomic systems only. As an extension of the previous work, a further elaboration of the projective stabilization method applied on holonomic and non-holonomic mechanical systems is reported in this paper.

2. UNCONSTRAINED MBS ON MANIFOLDS

Unconstrained multibody system (MBS) is an autonomous Lagrangian system. If n DOF is assumed, the system evolution in configuration space $\mathcal{R}^n$ is described (by definition) by Lagrangian equations [4, 6]:

$$\frac{\mathrm{d}}{\mathrm{d}t}\left(\frac{\partial L}{\partial \dot{\mathbf{x}}}\right)-\frac{\partial L}{\partial \mathbf{x}}=\mathbf{\Gamma}^{*},\mathbf{M}(\mathbf{x})\ddot{\mathbf{x}}=\mathbf{Q}^{*}(\mathbf{x},\dot{\mathbf{x}},t) \quad . \tag{1}$$

By taking differentiable manifold approach, the configuration space $\mathcal{R}^n$ is considered to be a manifold $\mathcal{M}^n$ covered by coordinate system $\mathbf{x}(t)$ (in mathematical jargon of modern differential geometry: locally covered by chart $\mathbf{x}$). The solution of (1) is a dynamical trajectory $\mathrm{T}: x^i = x^i(t)$ of the system in *n*-dimensional manifold of configuration $\mathcal{M}^n$. With every point on manifold of configuration, $\mathbf{x} \in \mathcal{M}$, the *n* dimensional tangent space $T_{\mathbf{x}}\mathcal{M}$ is affiliated, where system virtual displacements $\delta\mathbf{x}$ and velocities $\dot{\mathbf{x}}$ are contained, $\delta\mathbf{x} \in T_{\mathbf{x}}\mathcal{M}$, $\mathrm{d}\mathbf{x} \in T_{\mathbf{x}}\mathcal{M}$, $\dot{\mathbf{x}} \in T_{\mathbf{x}}\mathcal{M}$. The manifold $\mathcal{M}$ and the union of all tangent spaces at the various points $\mathbf{x}$ make another, 2*n*-dimensional, manifold called tangent bundle, $T\mathcal{M}: \bigcup_{\mathbf{x}\in\mathcal{M}^n} T_{\mathrm{x}}\mathcal{M}$, covered by the coordinates $\mathbf{x}, \dot{\mathbf{x}}: T\mathcal{M} = \{ (\mathbf{x}, \dot{\mathbf{x}}): \mathbf{x} \in \mathcal{M},\ \dot{\mathbf{x}} \in T_{\mathbf{x}}\mathcal{M} \}$ [4] (being mathematically not very rigorous, tangent bundle can be observed as a velocity phase space known from 'traditional' approach). Manifold $\mathcal{M}$ is not a vector space. By adopting system generalized mass matrix $\mathbf{M}(\mathbf{x})$ (positive definite) as a Riemannian metric on the manifold of configuration [7], a scalar product in each tangent space $T_{\mathbf{x}}\mathcal{M}$ is given by $\langle \mathbf{y}, \mathbf{z} \rangle_{\mathbf{M}(\mathbf{x})} = \mathbf{y}^{\mathrm{T}}\mathbf{M}(\mathbf{x})\mathbf{z}$, $\mathbf{y}, \mathbf{z} \in T_{\mathbf{x}}\mathcal{M}$. Now, with the metric so defined, the tangent space $T_{\mathbf{x}}\mathcal{M}$ ('the fiber of the tangent bundle at point $\mathbf{x}$') becomes a local Euclidean vector space spanned by covariant basis $\hat{\mathbf{g}}_{\mathbf{x}_i}$. By introducing a reciprocal contravariant basis $\hat{\mathbf{g}}_{\mathbf{x}}^i$ [4], the vectors in tangent spaces can be expressed using their contravariant and covariant representations $\hat{\dot{\mathbf{x}}} = \dot{x}^i\, \hat{\mathbf{g}}_{\mathbf{x}_i}$, $\dot{\mathbf{x}} = [\dot{x}^i]$, $\hat{\dot{\mathbf{x}}} = \dot{x}_i\, \hat{\mathbf{g}}_{\mathbf{x}}^i$, $\dot{\mathbf{x}}^* = [\dot{x}_i]$, $\mathbf{G}_{\mathbf{x}} = [\hat{\mathbf{g}}_{\mathbf{x}_1}, ..., \hat{\mathbf{g}}_{\mathbf{x}_n}]^{\mathrm{T}}$. The infinitesimal distance between two points on manifold (system kinematical line element) is defined by $\mathrm{d}s^2 = g_{ij}\mathrm{d}x^i\mathrm{d}x^j$, $\mathbf{M}(\mathbf{x}) = [g_{ij}]$. Being dependent both on $\mathbf{x}$ and $\dot{\mathbf{x}}$, the system kinetic energy $Ek(\mathbf{x}, \dot{\mathbf{x}}): T\mathcal{M}^n \to \mathcal{R}$ is defined on tangent bundle $T\mathcal{M}^n$. It is a quadratic, positive definite form on each tangent space: $Ek = \frac{1}{2}\|\dot{\mathbf{x}}\|^2_{\mathbf{M}(\mathbf{x})} = \frac{1}{2}\dot{\mathbf{x}}^{\mathrm{T}}\mathbf{M}(\mathbf{x})\dot{\mathbf{x}}$, $\dot{\mathbf{x}} \in T_{\mathbf{x}}\mathcal{M}$.

By following a standard procedure, Lagrangian equations (1) represent mathematical model in minimal form, which can be turned into the 2*n* ODE form:

$$\dot{\mathbf{v}} = \mathbf{M}^{-1}(\mathbf{x})\mathbf{Q}^*(\mathbf{x}, \mathbf{v}, t)\ ,\ \dot{\mathbf{x}} = \mathbf{v}\ ,\ \overline{\mathbf{x}} = \begin{bmatrix} \mathbf{x} \\ \mathbf{v} \end{bmatrix},\ \dot{\overline{\mathbf{x}}} = \mathrm{f}(\overline{\mathbf{x}})\quad ,\quad \mathrm{f}(\overline{\mathbf{x}}) = \begin{bmatrix} \mathbf{v} \\ \mathbf{M}^{-1}\mathbf{Q}^* \end{bmatrix}. \tag{2}$$

The solution of (2) is integral curve of the vector field $\mathrm{f}(\overline{\mathbf{x}})$ on tangent bundle ('velocity phase space') for a set of Cauchy data $(t_0, \overline{\mathbf{x}}_{\mathbf{0}})$.

3. GEOMETRIC PROPERTIES OF CONSTRAINTS

$$\mathbf{\Phi}(\mathbf{x}, t) = \mathbf{0}\,, \mathbf{\Phi}(\mathbf{x}, t): \mathcal{R}^n \times \mathcal{R} \to \mathcal{R}^r\quad , \tag{3}$$

Holonomic constraints (3), which are imposed on the system, restrict system configuration space and impose constraints at velocity level: a trajectory $\mathrm{T}: x^i = x^i(t)$ is 'forced to move' on the *n-r* dimensional constraint manifold $\mathcal{S}^{n-r}(t)$, $\mathcal{S}^{n-r}(t) = \{ \mathbf{x} \in \mathcal{M}, \Phi(\mathbf{x}, t) = \mathbf{0} \}$, $t \geq 0$, $\mathbf{x}(t_0) \in \mathcal{S}^{n-r}(t_0)$ and linear constraint equation (4) is induced at system velocities:

$$\mathbf{\Phi}^*{}_{\mathbf{x}}(\mathbf{x}, t)\dot{\mathbf{x}} = -\mathbf{\Phi}_t = \boldsymbol{\tau}\ . \tag{4}$$

If constraints are scleronomic, i.e. $\mathbf{\Phi}(\mathbf{x}) = \mathbf{0}$, the constraints at velocities take a form $\mathbf{\Phi}^*{}_{\mathbf{x}}(\mathbf{x})\dot{\mathbf{x}} = \mathbf{0}$, which determine $\hat{\dot{\mathbf{x}}}$ as a tangent to the position constraint manifold,

$\operatorname{rank}(\boldsymbol{\Phi}^{*}_{\mathbf{x}} = \dfrac{\partial \boldsymbol{\Phi}(\mathbf{x})}{\partial \mathbf{x}}) = r$. The system is said to be a holonomic one and posses *n-r* degrees of freedom (DOF). The constraint matrix $\boldsymbol{\Phi}^{*}_{\mathbf{x}}(\mathbf{x},t)$ can be written in the form $\boldsymbol{\Phi}^{*\mathrm{T}}_{\mathbf{x}}(\mathbf{x},t) = \left[\boldsymbol{\varphi}^{*}_{1},....,\boldsymbol{\varphi}^{*}_{r}\right]$, $\boldsymbol{\varphi}^{*}_{i} = \left[\varphi_{i}\right]$, $\hat{\boldsymbol{\varphi}}_{1} = \varphi_{i}\,\hat{\mathbf{g}}^{i}_{\mathbf{x}}$. The vectors $\hat{\boldsymbol{\varphi}}_{1},...,\hat{\boldsymbol{\varphi}}_{r}$ represent gradients to the constraint 'hyper-surfaces', determined in the configuration space by the equations $\boldsymbol{\Phi}(\mathbf{x},t) = \mathbf{0}$, i.e. $\hat{\boldsymbol{\varphi}}_{1} = \left[\operatorname{grad}\Phi_{1} = 0\right]$, … , $\hat{\boldsymbol{\varphi}}_{r} = \left[\operatorname{grad}\Phi_{\mathrm{r}} = 0\right]$. The vectors $\boldsymbol{\varphi}^{*}_{i}$ are linearly independent and span *r* dimensional constraint subspace $C^{r}_{\mathbf{x}}$ [2]. Kinematically admissible virtual displacements $\delta\mathbf{x}$ are restricted to the *n-r* dimensional tangent space $T_{\mathbf{x}}\mathcal{S}^{n-r}$ that is orthogonal to $C^{r}_{\mathbf{x}}$. Together, subspaces $C^{r}_{\mathbf{x}}$ and $T_{\mathbf{x}}\mathcal{S}^{n-r}$ span fiber of tangent bundle of unconstrained system $T_{\mathbf{x}}\mathcal{M}^{n}$ (tangent space) at point $\mathbf{x}$: $T_{\mathbf{x}}\mathcal{S}^{n-r} \cap C^{r}_{\mathbf{x}} = 0$, $T_{\mathbf{x}}\mathcal{S}^{n-r} \cup C^{r}_{\mathbf{x}} = T_{\mathbf{x}}\mathcal{M}^{n}$. Thus, orthogonal-complement matrix $\mathbf{R}(\mathbf{x},t)$, $\mathbf{R}(\mathbf{x},t) = \left[\mathbf{r}_{1},.....\mathbf{r}_{n-r}\right]$, that satisfy complementary equation $\boldsymbol{\Phi}^{*}_{\mathbf{x}}(\mathbf{x},t)\mathbf{R}(\mathbf{x},t) = \mathbf{0}$, can be determined where $\hat{\mathbf{r}}_{1},.....,\hat{\mathbf{r}}_{n-r}$ are basis vectors of $T_{\mathbf{x}}\mathcal{S}^{n-r}$ [1]. In the case of scleronomic constraints, system velocities (not just system virtual displacements $\delta\mathbf{x}$) are entirely contained in $T_{\mathbf{x}}\mathcal{S}^{n-r}$ and can be expressed with respect to the basis $\mathbf{G}_{\mathbf{r}} = \left[\hat{\mathbf{r}}_{1},.....,\hat{\mathbf{r}}_{n-r}\right]^{\mathrm{T}}$ only, i.e. $\hat{\dot{\mathbf{x}}} = \dot{\mathbf{z}}^{\mathrm{T}}\mathbf{G}_{\mathbf{r}}$, $\dot{\mathbf{x}} = \mathbf{R}\,\dot{\mathbf{z}}$, where system velocities are represented *via* independent generalized velocities $\dot{\mathbf{z}}$ (instead of representation $\hat{\dot{\mathbf{x}}} = \dot{\mathbf{x}}^{\mathrm{T}}\mathbf{G}_{\mathbf{x}}$ that is expressed *via* basis $\mathbf{G}_{\mathbf{x}}$ that 'covers' whole unconstrained tangent space $T_{\mathbf{x}}\mathcal{M}^{n}$). If the constraints are rheonomic (constraints do depend explicitly on time, a costraint manifold $\mathcal{S}^{n-r}$ 'moves' within $\mathcal{M}^{n}$), the velocities are not totally sunk in $T_{\mathbf{x}}\mathcal{S}^{n-r}$ and can be expressed *via* $T_{\mathbf{x}}\mathcal{S}^{n-r}$ basis and additional vector $\boldsymbol{\alpha}(\mathbf{x},t)$ according to the equation $\dot{\mathbf{x}} = \mathbf{R}\dot{\mathbf{z}} + \boldsymbol{\alpha}(\mathbf{x},t)$. The further time derivative yields equation $\ddot{\mathbf{x}} = \mathbf{R}\ddot{\mathbf{z}} + \dot{\mathbf{R}}\dot{\mathbf{z}} + \dot{\boldsymbol{\alpha}}(\mathbf{x},t)$ by means of which accelerations are constrained.

If, beside *h* holonomic constraints (3), the additional *nh* non-holonomic constraints in the form $\Psi(\mathbf{x},\dot{\mathbf{x}},t) = \mathbf{0}$ are imposed on the system:

a) they do not restrict system configuration space (system constraint manifold $\mathcal{S}^{n-r}$ maintains the same dimension, $r = h$),

b) they impose additional velocity constraints on holonomic constraint manifold tangent bundle $T\mathcal{S}$, $\dot{\mathbf{x}} \in T^{n-r-nh}_{\mathbf{x}}\mathcal{S}^{n-r} \subset T^{n-r}_{\mathbf{x}}\mathcal{S}^{n-r}$.

If non-holonomic constraints are linear in velocities, i.e. can be given in Pfaffian form $\boldsymbol{\Psi} = \mathbf{B}^{*}(\mathbf{x},t)\dot{\mathbf{x}} - \boldsymbol{\beta}(\mathbf{x},t) = \mathbf{0}$, the system constraint equations can be written as follows:

$$\begin{bmatrix}\boldsymbol{\Phi}^{*}_{\mathbf{x}}(\mathbf{x},t)\\ \mathbf{B}^{*}(\mathbf{x},t)\end{bmatrix}\dot{\mathbf{x}} = \begin{bmatrix}\boldsymbol{\tau}\\ \boldsymbol{\beta}\end{bmatrix},\ \begin{bmatrix}\boldsymbol{\Phi}^{*}_{\mathbf{x}}(\mathbf{x},t)\\ \mathbf{B}^{*}(\mathbf{x},t)\end{bmatrix} = \boldsymbol{\Phi}^{*}_{\mathbf{x}nh}\ ,\ \boldsymbol{\Phi}^{*}_{\mathbf{x}nh} \in \mathcal{R}^{h+nh\times n} \tag{5}$$

As it was the case with systems that posses only holonomic constraints, the orthogonal-complement matrix $\mathbf{R}_{nh}$ that satisfy complementarity equation $\boldsymbol{\Phi}^{*}_{\mathbf{x}nh}\mathbf{R}_{nh} = \mathbf{0}$ can be determined *via* numerical methods described in literature [2, 3].

4. CONSTRAINT GRADIENT PROJECTIVE METHOD FOR STABILIZATION OF CONSTRAINT VIOLATION

If system governing equations are based on the mathematical models in descriptor form [3], a constraint violation stabilization method have to be applied during integration procedure. The

stabilization algorithm proposed in [3] is based on the projection of system state-point after integration step to the constraint manifold in the course of simulation. If constraint violation (specified by given numerical tolerances) occurs after step-integration phase, the 'position' stabilization step is to be performed by correcting dependent coordinates sub-vector $\mathbf{x}^{\mathrm{d}}$ *via* solving system constraint equation (3), providing thus shifting of the system state-point $\mathbf{x}$ back to constraint manifold $\mathcal{S}^{n-r}$. The procedure is then repeated at the velocity level by correcting $\dot{\mathbf{x}}^{\mathrm{d}}$ to bring $\dot{\mathbf{x}}$ in accordance with (4). As stabilization step final result, time-integration values $\dot{\mathbf{x}}, \mathbf{x}$ are projected to the constraint manifold tangent bundle $T\mathcal{S}$, thus completely satisfying constraints of the system. As will be seen later, a crucial point of the algorithm is appropriate selection of sub-vectors $\mathbf{x}^{\mathrm{d}}$ and $\dot{\mathbf{x}}^{\mathrm{d}}$ to provide the optimal stabilization effect. Criteria for the coordinates selection can be expressed geometrically: basically, every selection that returns sub-vector of dependent coordinates $\mathbf{x}^{\mathrm{d}}$ whose basis vectors have non-zero projections on the constraint subspace $\mathcal{C}^r_{\mathbf{x}}$ (corresponding $r \times r$ sub-matrix of constraint matrix $\mathbf{\Phi}^*{}_{\mathbf{x}}$ is non-singular) is correct one and can be used for stabilization procedure. Consequently, the basis vectors of variables $\mathbf{x}^{\mathrm{i}}$ have projections on tangent space of constraint manifold $T_{\mathbf{x}}\mathcal{S}^{n-r}$ that is complement to $\mathcal{C}^r_{\mathbf{x}}$. If the extracted sub-vectors do not satisfy specified conditions, the selection is not a valid one and the calculation will fail.

4.1. Stabilization of configuration constraints violation

The main problem that may occur during stabilization procedure is an inadequate coordinate selection that may have a negative effect on the integration accuracy along the constraint manifold. Although, as it was explained, every partitioning that returns acceptable sub-vectors can be used for stabilization, a non-optimal choice of the coordinate sub-vectors may cause an increase of the numerical errors along the manifold during stabilization part of the integration procedure. If this happens, a correction of the constraint violation will be accomplished at the expense of the 'kinetic motion' accuracy obtained by the system variables $\dot{\mathbf{x}}, \mathbf{x}$ ODE integrators. The 'mechanism' of emerging of numerical errors along configuration manifold, because of an inadequate partitioning during the stabilization procedure of holonomic systems, is outlined in Fig. 1, where an illustrative example $\mathbf{x} \in \mathcal{M}^2$, $\mathcal{S}^1$ is discussed.

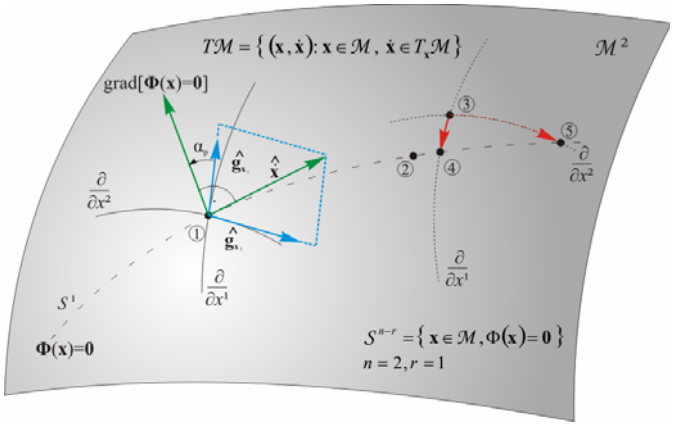

Figure 1. Numerical correction of configuration constraint violation

Assuming that, starting from ①, an integration of ODE gives result ③ instead of exact position ②, a projection on the constraint manifold $\mathcal{S}^1$ by adjusting coordinate x^1 (solving constraint equation (3) along x^1 curve) yields result ④ that is consistent to the constraint. If instead of x^1, the variable x^2 was chosen to be a dependent coordinate, an adjustment of the

integration result along x^2 curve would yield solution ⑤, which is also consistent to the constraint but contains considerable error along the manifold $\mathcal{S}^1$. A remedy for the problem of an inadequate selection of dependent coordinates has been described in [2], where a projective criterion to the coordinate partitioning method is discussed. The main idea is to determine those *r* coordinates whose direction vectors $\hat{\mathbf{g}}_{\mathbf{x}i}$ deliver the biggest relative projections to the $\boldsymbol{C}_{\mathbf{x}}^{r}$ (i.e. 'small' value of α_p) and select them as dependent variables which will be adjusted during the stabilization procedure. By correcting the coordinates whose direction vectors align well with the constraint gradients, it is ensured that the correction procedure will shift a state-point of the system 'as direct as possible' to the constraint 'hyper-surfaces', minimizing thus an error along constraint manifold.

4.2. Structure of partitioned sub-vectors

So far, constraint gradient projective method has been discussed for stabilization of constraint violation during numerical simulation of holonomic systems only [3]. Would it be possible to apply proposed algorithm in the framework of simulation procedures of non-holonomic systems? In the case of holonomic system, if partitioned sub-vector at the position level is selected, can the same sub-vector be used automatically for stabilization at the velocity level as well? Is it valid in any case? To get answers on these questions and gain further insight into described procedure, it is illustrative to observe characteristics of the proposed algorithm at the tangent bundle (6) of an unconstrained system:

$$T\mathcal{M} = \left\{ (\mathbf{x}, \dot{\mathbf{x}}) : \mathbf{x} \in \mathcal{M},\ \dot{\mathbf{x}} \in T_{\mathbf{x}}\mathcal{M} \right\} \quad . \tag{6}$$

As explained, $T\mathcal{M}$ is 2*n*-dimensional *Riemannian* manifold with a metric $\mathbf{M}_{T\mathcal{M}} = \mathrm{diag}(\mathbf{M}(\mathbf{x}), \mathbf{M}(\mathbf{x}))$, where system 'positions' as well as system velocities can be studied [6]. If holonomic constraints are present, they are represented in $T\mathcal{M}$ by sub-manifolds at configuration and velocity levels. These sub-manifolds determine the possible states of the system. By using the projective criterion for both sub-manifolds, the characteristics of the partitioning procedure that for a given set of coordinates $\mathbf{x} \in \mathcal{M}$, $\dot{\mathbf{x}} \in T_{\mathbf{x}}\mathcal{M}$ provides the optimal dependent/independent sub-vectors, can be learned as follows.

The configuration submanifold $\mathcal{S}^{n-r}$ is determined by the equation (3) i.e.

$$\mathcal{S}^{n-r} = \left\{ \mathbf{x} \in \mathcal{M}, \Phi(\mathbf{x}, t) = \mathbf{0} \right\} \quad , \tag{7}$$

The submanifold $\mathcal{V}^{n-r}$, by means of which the system velocities $\dot{\mathbf{x}}$ are constrained, is defined by (4), thus

$$\mathcal{V}^{n-r} = \left\{ \dot{\mathbf{x}} \in T_{\mathbf{x}}\mathcal{M}\ ,\ \Phi^{*}{}_{\mathbf{x}}(\mathbf{x}, t)\, \dot{\mathbf{x}} = \boldsymbol{\tau} \right\} \quad . \tag{8}$$

If constraint gradient projective method is to be applied for stabilization purposes at both levels, the projective criterion will be based on determination of the gradients to the constraint sub-manifolds $\mathcal{S}^{n-r}$ and $\mathcal{V}^{n-r}$ respectively (as explained, this is because the extraction of the dependent coordinates of $\mathbf{x}^{\mathrm{d}}$ and $\dot{\mathbf{x}}^{\mathrm{d}}$ depend on the directions of gradients to the 'hyper-surfaces' of sub-manifolds $\mathcal{S}^{n-r}$ and $\mathcal{V}^{n-r}$). Since constraint submanifold $\mathcal{S}^{n-r}$ is determined by (3), the $\mathbf{x}$ correction gradient by means of which $\mathbf{x}^{\mathrm{d}}$ is to be extracted is given by (9). Similarly, $\dot{\mathbf{x}}$ correction gradient for an extraction of $\dot{\mathbf{x}}^{\mathrm{d}}$ is determined by (10):

$$\mathrm{grad}\left[\boldsymbol{\Phi}(\mathbf{x}, t) = \mathbf{0}\right] = \boldsymbol{\Phi}_{\mathbf{x}}^{*}(\mathbf{x}, t) \quad , \quad \mathrm{grad}\left[\boldsymbol{\Phi}_{\mathbf{x}}^{*}(\mathbf{x}, t)\, \dot{\mathbf{x}} = \boldsymbol{\tau}\right] = \boldsymbol{\Phi}_{\mathbf{x}}^{*}(\mathbf{x}, t) \,. \tag{9),(10}$$

Now, if the expressions (9) and (10) are compared, it is obvious that the both hyper-surfaces $\mathcal{S}^{n-r}$ and $\mathcal{V}^{n-r}$ possess the same gradients for every point in $T\mathcal{M}$ (in fact, the both gradients depend on the current position $\mathbf{x} \in \mathcal{M}$ at the configuration manifold and *t* only, i.e. they are independent on system velocities $\dot{\mathbf{x}}$). Of course, this stems from the fact that, in the case of holonomic systems, the velocity submanifold $\mathcal{V}^{n-r}$ is determined by algebraic equations (4)

(linear in $\dot{\mathbf{x}}$!) which are, in turn, obtained by derivation of configuration constraints (3). Since the gradients to the both hyper-surfaces $\mathcal{S}^{n-r}$ and $\mathcal{V}^{n-r}$ are identical, which is valid also for directions of the basis vectors at both levels, it is clear that the same optimal dependent/independent sub-vectors for 'positions' and velocities will be extracted during the process. This means that, once the partitioning procedure is performed for optimal position sub-vector $\mathbf{x}^{\mathrm{d}}$, the algorithm is not needed to be repeated at the velocity level (the subvector $\dot{\mathbf{x}}^{\mathrm{d}}$ of the same structure is to be chosen for the stabilization of velocities).

A constraint gradient projective method can also be applied for stabilization of constraint violation of non-holonomic systems. As explained, if additional *nh* non-holonomic constraints are given in Pfaffian form, the submanifold $\mathcal{V}^{n-r-nh}$ of the velocity constraints is defined by (11), which yields velocity correction gradient in the form (12):

$$\begin{bmatrix} \boldsymbol{\Phi}_{\mathbf{x}}^{*}(\mathbf{x},t) \\ \mathbf{B}^{*}(\mathbf{x},t) \end{bmatrix} \dot{\mathbf{x}} = \boldsymbol{\Phi}_{nh}^{*} \dot{\mathbf{x}} = \begin{bmatrix} \boldsymbol{\tau} \\ \boldsymbol{\beta} \end{bmatrix}, \tag{11}$$

$$\operatorname{grad}\left[\boldsymbol{\Phi}_{nh}^{*} \dot{\mathbf{x}} = \begin{bmatrix} \boldsymbol{\tau} \\ \boldsymbol{\beta} \end{bmatrix} \right] = \boldsymbol{\Phi}_{nh}^{*}(\mathbf{x},t) = \begin{bmatrix} \boldsymbol{\Phi}_{\mathbf{x}}^{*}(\mathbf{x},t) \\ \mathbf{B}^{*}(\mathbf{x},t) \end{bmatrix} \quad . \tag{12}$$

Since non-holonomic constraints do not affect configuration manifold $\mathcal{S}^{n-r}$, the 'position' coordinates correction gradient is given by (9). By comparing correction gradients (9) and (12), it can be concluded that they do not match any more. Thus, in the case of non-holonomic systems the optimal coordinates partitioning will not 'return' dependent/independent subvectors of the same structure for configuration and velocity stabilization. Beside non-equality of dimension of the sub-vectors $\mathbf{x}^{\mathrm{d}} \in \mathcal{R}^{r}$ and $\dot{\mathbf{x}}^{\mathrm{d}} \in \mathcal{R}^{r+nh}$, their structure will also differ in general case. Generally, in the case of non-holonomic systems, a separate partitioning procedure is necessary for stabilization at configuration and velocity level. This is specially true if the imposed non-holonomic constraints are non-linear in velocities and can not be put in Pfaffian form.

5. NUMERICAL EXAMPLE

To illustrate characteristics of the projective stabilization method, when applied in the framework of dynamic simulation of non-holonomic systems, a numerical example of a snakeboard that has been controlled to move along the specified path, is presented in [5]. The snakeboard is modelled as multibody system with 4 bodies connected to each other by means of pin-joints. There is one coupler, two small boards with wheels and one rotor on the coupler to model dynamical excitation of human body torso motion. The two pairs of wheels cannot slide and therefore impose two non-holonomic constraints on the system. On the configuration level, the snakeboard possess 6 DOF (Fig. 2).

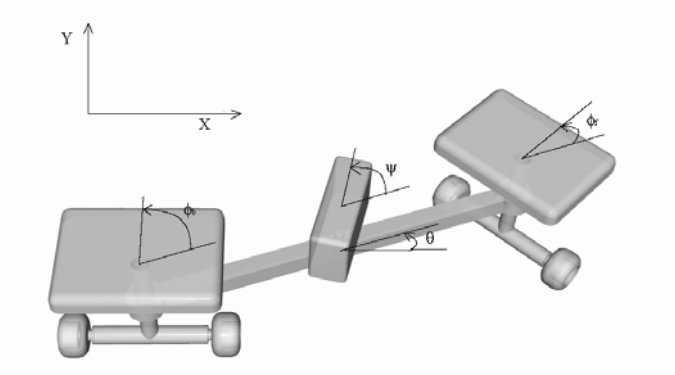

Figure 2. Non-holonomic mechanical system: snakeboard

To propel the snakeboard, a rider first needs to move his feet to get the wheels in an appropriate direction. By turning his torso (modeled here by the rotor mounted on the coupler), the snakeboard then moves according to the wheel angles. A simulation with such propulsion has been obtained with initial values $x = y = \phi_b = 0$, $\psi = 1.6\,\text{rad}$, $\theta = \pi/4\,\text{rad}$ and $\phi_f = 0.1\,\text{rad}$ and sinusoidal torques applied on the rotor and the wheel-boards. The frequency of the actuations is 1Hz and the simulation period is 2s.

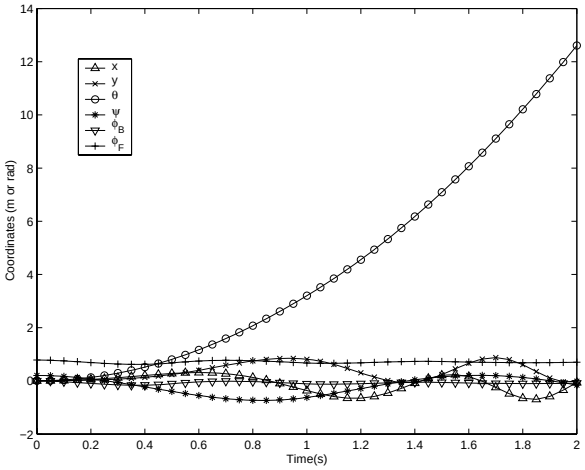

Figure 3. Evolution of the coordinates in time

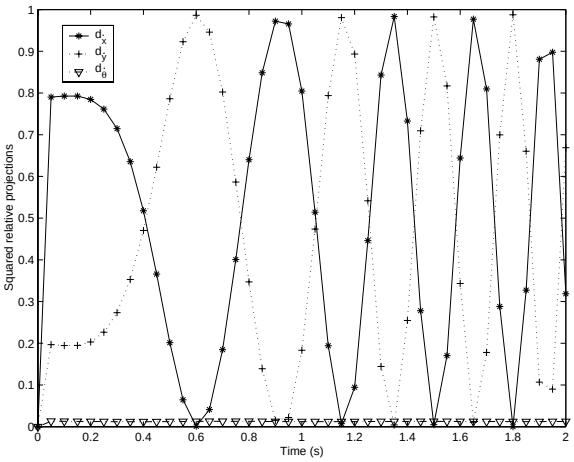

Figure 4. Evolution of the projections *d*

This results in a relatively slow motion along the *x*-axis (Fig. 2). The projective method has been applied on this simulation, but choice of the independent velocities for solving holonomic/non-holonomic velocity constraints did not to have a significant influence on the quality of the results. This is due to the small magnitudes of the velocities involved in the constraint equations.

To demonstrate the effect of the projective stabilization method, a different numerical case is discussed in the sequel. This case-study describes a less natural motion, as actuation is provided by a force $\mathbf{f} = \begin{pmatrix} f_x & f_y \end{pmatrix}$ with constant amplitude acting on the centre of mass of the snakeboard and varying orientation parallel to the coupler, towards the front wheels. Springs with a constant of 0.1 Nm/rad are added at the wheel boards to keep the initial relative angles between wheels and coupler. Another spring with a constant of 1 Nm/rad has also been added between the coupler and the rotor. The initial values are $x = y = \theta = \phi_b = 0$, $\psi = 0.2\,\text{rad}$ and $\phi_f = \pi/3\,\text{rad}$.

The simulation has been run under 4 different ODE numerical integrations. First, an Runge-Kutta (4,5) algorithm with variable stepsize was used, to obtain a reference simulation S1 (Fig. 3). The absolute and relative tolerances were set to 1e-13. To test the stabilization procedures, the equations of motion have subsequently numerically integrated without stabilization (S2), with stabilization using the optimal choice of independent coordinates (S3) and with stabilization using an other possible choice of independent coordinates (S4). For these simulations, a fourth order Runge-Kutta integration scheme was used with a fixed stepsize of 0.01 seconds. In this simulation, the snakeboard performs a circular motion.

The velocities $\dot{\psi}$, $\dot{\phi}_b$ and $\dot{\phi}_f$ do not appear in the two constraint equations and are therefore independent. The fourth independent coordinate for simulation S3 was chosen amongst $\dot{x}$, $\dot{y}$ and $\dot{\theta}$ using the projective criterion. The squared relative projections d of the direction vectors on the tangent subspace are shown on Figure 4. For simulation S3, the biggest projection was used to choose the independent velocity, it was alternatively $\dot{x}$ and $\dot{y}$.

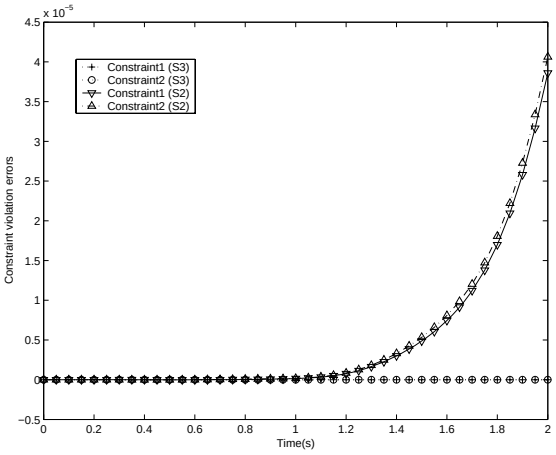

Figure 5. Constraint violation errors

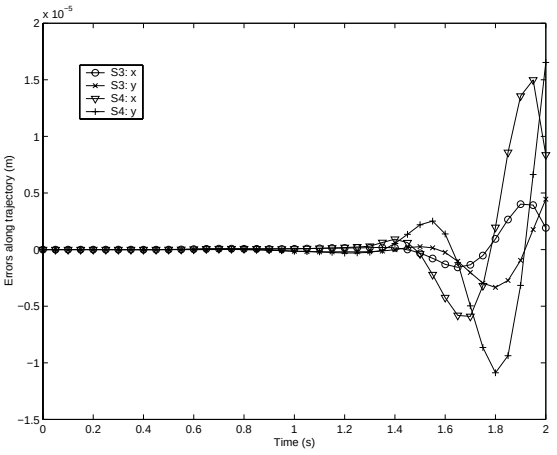

Figure 6. Errors along trajectories.

In Figure 5, the constraint violations errors are shown for the simulations cases with and without stabilization of the constraint violation errors (S2), (S3). It is shown that for the stabilized (S3) case, the errors are theoretically zero. For the simulation without stabilization, we see growing of violation errors. During simulation (S4), the second biggest projection (Fig. 4) was used as the independent velocity. Although this choice is valid and eliminates the constraint violation errors, it is not optimal one and it introduces larger errors along the trajectory (Fig. 6). Of course, the propagation of these errors may be attempted to be controlled by tuning ODE integrator numerical parameters, but Fig. 6 shows a typical situation with non-optimized partitioning choice.

6. CONCLUSION

The issues of geometric and stabilization characteristics of the constraint gradient projective method, which has been used as the stabilization procedure within time-integration method proposed in [3], have been addressed in the paper. By adopting differential-geometric point of view, a 'mechanism' of emerging of numerical errors along the 'position' configuration manifold during projection step have been discussed, along with the issue of stabilization of the constraints at the velocity level. In the case of simulation of holonomic systems, the optimal coordinate partitioning returns sub-vectors of the same structure at the both position and velocity level. Generally, in the case of non-holonomic systems, the constraint gradient projective method should be performed separately for each stabilization level. This is specially true if the imposed non-holonomic constraints can not be put in Pfaffian form.

REFERENCES

[1] W. Schiehlen, Multibody System Dynamics: Roots and Perspectives, *Multibody System Dynamics*, **1**, 149-188 (1997).

[2] W. Blajer, Elimination of Constraint Violation and Accuracy Aspects in Numerical Simulation of Multibody Systems, *Multibody System Dynamics*, **7**, 265-284 (2002).

[3] Z. Terze, D. Lefeber, O. Muftić, Null Space Integration Method for Constrained Multibody System Simulation with no Constraint Violation, *Multibody System Dynamics*, **6**, 229-243 (2001).

[4] R. Abraham et al, *Manifolds, Tensor Analysis, and Applications*, Springer-Verlag, New York (1988).

[5] Z. Terze et al, Constraint Gradient Projective Method for Stabilized Dynamic Simulation of Constrained Multibody Systems*, ASME 19th Bien. Conference on Mech. Vibration and Noise*, Chicago, USA, 2003.

[6] B. F. Shutz, *Geometrical Methods of Mathematical Physics*, Cambridge Univ. Press, Cambridge, 1980.

[7] U. Jungnickel, Differential-Algebraic Equations in Riemannian Spaces and Applications to Multibody System Dynamics, *Zeitschrift fuer Angewandte Mathematik und Mechanik*, 74, 409-415 (1994).

Prof. dr. sc. Zdravko Terze
Univ. of Zagreb, F. of Mech. Eng. And Naval Arch., Dept. of Aerospace Eng., Zagreb, zdravko.terze@fsb.hr
Joris Naudet, PhD
Vrije Universiteit Brussel, Dept. of Mech. Eng., Multibody Mechanics Group, joris.naudet@vub.ac.be